Optimal Photovoltaic System Design with Multi-objective Optimization

Amin Ibrahim, University of Ontario Institute of Technology, Canada
Farid Bourennani, University of Ontario Institute of Technology, Canada
Shahryar Rahnamayan, University of Ontario Institute of Technology, Canada
Greg F. Naterer, Memorial University of Newfoundland, Canada

ABSTRACT

Recently, several parts of the world suffer from electrical black-outs due to high electrical demands during peak hours. Stationary photovoltaic (PV) collector arrays produce clean and sustainable energy especially during peak hours which are generally day time. In addition, PVs do not emit any waste or emissions, and are silent in operation. The incident energy collected by PVs is mainly dependent on the number of collector rows, distance between collector rows, dimension of collectors, collectors inclination angle and collectors azimuth, which all are involved in the proposed modeling in this paper. The objective is to achieve optimal design of a PV farm yielding two conflicting objectives namely maximum field incident energy and minimum of the deployment cost. Two state-of-the-art multi-objective evolutionary algorithms (MOEAs) called Non-dominated Sorting Genetic Algorithm-II (NSGI-II) and Generalized Differential Evolution Generation 3 (GDE3) are compared to design PV farms in Toronto, Canada area. The results are presented and discussed to illustrate the advantage of utilizing MOEA in PV farms design and other energy related real-world problems.

Keywords: *PV collector arrays, multi-objective optimization, NSGA-II, GDE3, renewable energy.*

1. INTRODUCTION

Solar energy is one of the most widely used renewable energies; because it is emission free and it is easily deployable. Several sun-based energy generation methods exist, such as, photovoltaic farms (PV), concentrated solar power plants, and solar thermal electricity plants. These systems can be used for meeting the global energy crisis due to rising world-wide demands and insufficient supply of electricity throughout the world by deploying the appropriate systems in the required areas. For example, PV are inefficient in very hot areas, such as desert, but are more efficient in mild to cold areas. In this paper, PV panels are selected because of mild-cold weather conditions in Canada. Although Canada produces enough electricity to fulfill the national demand, nevertheless solar energy is of special interest due to PV non-polluting properties.

Concentrated solar systems like the parabolic trough heat transfer fluid/steam systems can typically generate full rated electrical output for 10-12 hours a day

(Schlaich et al., 2005). Other solar power generation systems include large solar updraft towers which can produce large amounts of electricity via utilizing air flow created by heated air which drives pressure staged turbines (Price et al., 2002). In spite of these available large-scale technologies, photovoltaic panels are the most popular method of harvesting solar energy, because they directly convert the Sun's rays into electrical power. In addition, photovoltaic panels can be deployed anywhere and can provide a relatively stable electrical output. However, there are several drawbacks; they are subject to changing output efficiencies based on external factors such as shade, cloudy weather, covered by sands, and others.

Photovoltaic systems consist in converting solar radiation (sunlight) directly to electricity. There are two types of solar radiations on the Earth: direct and diffuse radiations. The sunlight is filtered through the Earth's atmosphere. Then, the solar radiation is received directly from the Sun without having been dispersed by the atmosphere is called direct radiation. When the sun's radiation is changed by the atmosphere due to clouds, water vapor, and other molecules, it is called *diffuse* radiation. Therefore energy absorbed by the PV panels are the sum of the amount of direct and diffuse radiations received in a given day.

In this paper, we propose the use of two state-of-the-art MOEAs, namely, NSGA-II and GDE3 to optimize the deployment of solar PV farms. The objectives consisted in maximizing the total incident solar energy and minimizing the cost of PV panel deployment in a specific field. As in Refs. (Sheskin, 2007) and (Talbi, 2009), the cost was limited to initial investment because the paper focused only on the PV configuration setup. However, a real PV farm requires overhead costs such as maintenance costs, residual fees, energy storage component fee and others. Six decision variables composed the optimization problem, namely, the number of collector rows, the distance among collector rows, the dimension of collectors, the collectors inclination angle, and the collectors azimuth angle.

The remainder sections of this paper are organized as follows: Related work, description of the designed mathematical model of PV panels, the description of the two algorithms used in this experiment and their fixed settings of the control parameters, the experimental results, and conclusions. In the Appendix A section can be found the list of symbols used in this paper, and Appendix B provides the monthly averaged direct beam and diffuse irradiance, monthly averaged hourly solar and azimuth angles due south in Toronto.

In the last few decades, there has been a large number of studies on single-objective and multi-objective real-life applications (Talbi, 2009). However, most real-life problems are multi-objective problems by nature because they involve variant conflicting objectives. The development of efficient multi-objective metaheuristics such as evolutionary multi-objective algorithms played an integral role in the design of complex energy systems. This section presents the most recent optimization works applied to design solar energy systems.

Varun (Varun, 2010) implemented a genetic algorithm for maximizing the thermal performance of flat plate solar air heaters to optimize various systems and operating parameters. The basic values like number of glass covers, Irradiance and Reynolds, plate tilt angle, and emissivity of plate are optimized for maximizing thermal performance.

Thiaux et al. (Thiaux et al., 2010) applied NSGA-II algorithm to optimize the load profile impact on stand-alone photovoltaic system gross energy

requirement. Yang et al. (Yang et al., 2007) developed a hybrid optimized solar-wind system. They optimized the components' capacity sizes of hybrid solar-wind power generation systems which employs a battery bank. Chang (Chang, 2010) attempted to maximize the electrical energy output of photovoltaic modules using a hybrid heuristic method. They combined PSO with nonlinear time-varying evolution to determine the optimal tilt angle of the modules.

Recently, Deb et al. (Deb et al., 2012) have attempted to solve a four-objective optimization model of a solar thermal power plant operation system. The four objectives were profit, total investment costs, internal rate of return, and pollution. First, they have used clustered NSGA-II algorithm to find set of trade-off solutions over the entire Pareto-optimal front. Then, they used a reference point based on Multiple Criterion Decision Making (MCDM) approach with the clustered NSGA-II to find preferred solutions on some parts of the Pareto-optimal front. They have demonstrated multi-objective optimization procedure with user decision making interaction to find a single preferred solution.

Mellit et al. (Mellit et al., 2009) describes the effect of utilizing various models and artificial intelligence based design methods to increase the efficiency of solar-wind hybrid plants. The proposed system was specially efficient for rural and isolated areas which suffer from lack of meteorological data due the limited weather station, a simulation method is used for completing the missing data.

In a related study, the shading among solar panels was modeled and a simulation-based algorithm was developed to predict the loss of energy due to shade in three individual locations in Arizona (Sadineni et al., 2008). Myers et al. (Myers et al., 2010) have proposed and simulated a theoretical solar cell by using a modified genetic optimization algorithm for shaping solar cells. The result of the optimization process is a 3D shape which fits within the area and volume of a conventional solar cell but it is drastically more efficient than regular rectangular shapes.

O. Ekren and Y. Ekren (Ekren and Ekren, 2010) have used simulation and single-solution based metaheuristic algorithm, called simulated annealing (SA), for optimizing the size of a PV-wind integrated hybrid energy system with battery storage. The objective function was the minimization of the hybrid energy system's total cost. They have demonstrated that the optimum result obtained by the SA algorithm showed a 10.13\% improvement on the objective function as compared to their simulation model.

Appelbaum and Weinstock (Appelbaum & Weinstock, 2004) worked on electrical output maximization for photovoltaic farms by concentrating on shading and spacing issues. They employed the Sequential Quadratic Programming for optimization. More recently, they added the azimuth angle of a solar panel as a new variable to the problem (Appelbaum & Weinstock, 2009). However, the variable is manipulated in a manual fashion while the system is optimized automatically. They reached 12\% in efficiency enhancement for a small scale photovoltaic array by reducing the amount of shading. Bourennani et al. (Bourennani et al., 2001). utilized Differential Evolution (DE) and simulation-based optimization methods to compare the maximum annual incident energy captured by the solar collectors. The captured energy was similar between the simulation approach and DE.

This paper is inspired from (Bourennani et al., 2001), (Appelbaum & Weinstock, 2004 & 2009) works; however, the problem was transformed into a multi-

objective problem. To the best, of our knowledge, this paper is the first to optimize the configuration setup of PV panels by optimizing multiple objectives. Rarely multi-objective optimization methods were used in PV field. Ref. (Thiaux, 2010) used MOO but they focused on the optimization of the entire solar farm assuming a certain static setup whereas this paper focuses on the setup of PV panels which is composed of six decision variables namely, the number of collector rows (a discrete variable), distance among the collector rows, the inclination of the PV panels, the height of a PV panel, collector's azimuth due south, and collector's clearance above ground. Two evolutionary multi-objective algorithms are used to for optimization, namely NSGA-II and GDE3. The results are compared and discussed in detail.

2. PHYSICAL SYSTEM MODEL

The model to be optimized is composed of stationary PV panels. The objective is to capture the maximum solar radiation with minimal cost investment. The PV collectors are fixed in the field as shown in Fig. 1. As it can be seen, the collectors are inclined at an angle β facing roughly the south. The dimension of the collectors is referred as length L and as height H. The length of the collectors L is equal to the length of the field whereas the width is W. There should be a minimum clearance of E above the ground to minimize the collectors of dust, debris, or snow.

2.1 Solar Collector Model

Collector maintenance requires the height of them above the ground to be limited. Also, the minimum distance, D between two rows is limited to allow easy access between PV panels. Moreover, the height H of the collectors themselves is limited by the manufacturer (Appelbaum & Weinstock, 2004 & 2009). Thus,

$$H' + E \leq A_{max} \quad (1)$$

$$H \leq H_{max} \quad (2)$$

where $H' = Hsin\beta$.

The configuration factors for un-shaded and shaded are given by as follow, respectively:

$$F_d = cos^2\left(\frac{\beta}{2}\right) \quad (3)$$

$$F_d^{sh} = F_d - \left[(d^2+1)^{\frac{1}{2}} - d\right] sin\beta \quad (4)$$

where d is the normalized distance between two rows given by $d = D/H'$.

Figure 1. Collectors arrangement in a stationary solar field, K indicates row number, L indicates length of PV, W indicates the width of the solar field, D indicates the distance between collector rows, β indicates PVs' inclination angle, and H' indicates the perpendicular distance created by the PVs.

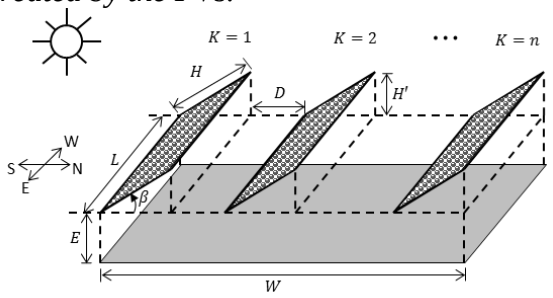

The incidence angle θ is the angle between a normal to the collector face and the incoming solar beam and it depends on the sun angles (altitude and azimuth) and collector angles (azimuth and tilt, Fig. 2).

$$\cos\theta = \cos\beta\sin\alpha + \sin\beta\cos\alpha\cos\gamma \quad (5)$$

Where α is the sun elevation angle; β is the collector inclination angle and $\gamma = \gamma_S - \gamma_C$

is the difference between the sun and collector azimuth with respect to south.

The relative shaded area is calculated by:

$$a_s = \frac{l_s}{L} \times \frac{h_s}{H} \quad (6)$$

Figure 2. Incidence angle θ: angle between a normal to the collector face and the incoming solar beam.

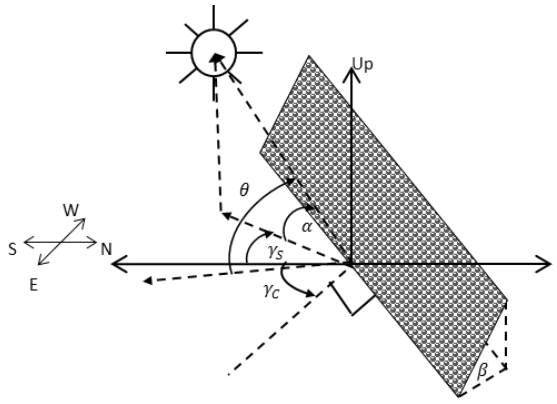

Where,

$$l_s = 1 - \frac{d\sin\beta+\cos\beta}{l} \times \frac{|\sin\gamma|}{\cos\beta\sin\alpha+\sin\beta\cos\gamma} \quad (7)$$

and

$$h_s = \frac{dsin\beta+cos\beta}{cos\beta+\frac{sin\beta cos\gamma}{tan\alpha}} \quad (8)$$

$l = L/H'$ is the normalized collector length.

The yearly direct (q_b) and diffuse (q_d) beam irradiation per unit area of an un-shaded collector (first row) are calculated by:

$$q_b = \sum_{n=1}^{n=365} \sum_{T_R}^{T_S} G_b \cos\theta \ \Delta T \quad (9)$$

and

$$q_d = F_d \sum_{n=1}^{n=365} \sum_{T_R}^{T_S} G_{dh} \Delta T \quad (10)$$

The the average yearly direct (q_b^{sh}) and diffuse (q_d^{sh}) beam irradiation per unit area of an un-shaded collector $((K-1)$ row) are given by:

$$q_b^{sh} = \sum_{n=1}^{n=365} \sum_{T_R}^{T_S} G_b \cos\theta \ (1 - a_s)\Delta T \quad (11)$$

and

$$q_d^{sh} = F_d^{sh} \sum_{n=1}^{n=365} \sum_{T_{SR}}^{T_{SS}} G_{dh} \Delta T \quad (12)$$

where ΔT is the summation time interval from sun rise T_R to sunset T_S on the collector for the beam irradiance, and from sun rise T_{SR} to sun set T_{SS} for the diffuse irradiance. The outer summation represents one year term from January 1st $(n = 1)$ to December 31st $(n = 365)$. Fig. 3 shows the sixth decision variable (γ_C); collectors azimuth with respect south and limited to $[-45^o, 45^o]$.

Figure 3. Collector azimuth with respect to south (γ_C).

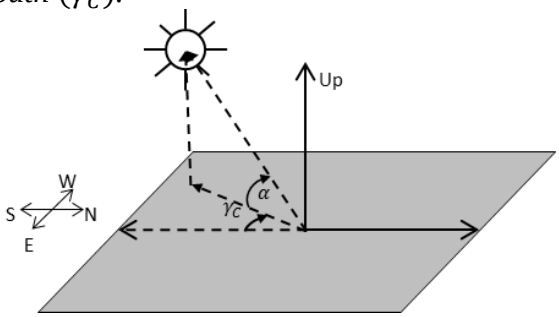

2.2 System Complexities

The current multi-objective optimization PV farm design is composed of several complexities that make it hard to solve. It is composed of mixed-type integer and real variables. The first objective is multimodal because it encompasses trigonometric functions which are hard to solve. The Pareto front geometry is convex composed in majority of a linear component and a curved convexity at the extreme as shown in Fig. 6. Some variables take widely different ranges of values, thereby making it difficult for the solvers to provide adequate emphasis to correct variable combinations. Despite the existence of only six variables (6D), this problem exhibits a wide and non-uniform range of variable values. In addition, the

non-dominated solutions' variables are composed of other complexities which are a) non-extremal and b) non-medial having a c) dissimilar parameter domains and d) many-to-one mappings which make the problem more complicated to solve (Huband et al., 2006). Dissimilar parameter domains consists in having variables with completely dissimilar parameters domain; for example, the height and inclination angle are defined as follows $0.2 \leq H \leq 2$ and $0^o \leq \beta \leq 90^o$. Many-to-one mappings imply that different combination of parameters can generate exactly the same solutions (same fitness values). For example, in Figs. 6 and 7 you can see on the Pareto front two solutions one after the other totally different. One solution has six rows of PV panels with small dimensions and the next one has only two rows with very large panel dimensions. Both cases result roughly in the same cost and the energy generation.

2.3 Objectives, Variables, and Constraints

The optimization problem is composed of two objectives, six variables, and two constraints. A final optimal solution is composed of the following variables: the number of collector rows, distance between collector rows, dimension of collectors, collectors inclination angle, and collectors azimuth angle. The objectives, constraints, and variable domains are described below in equations 13 to 22.

The two objectives are the maximization of incident energy and minimization of the installation and material cost.

1) Incident energy: the yearly absorbed incident energy should be maximized in order to generate the maximum possible electricity.
2) Cost: the cost of PV array collectors installation should be as low as possible.

The mathematical formulation of the optimization problem is defined as follows:

$$\max \mathrm{Q} = K \times L \times \left[q_b + q_d + (K-1)\left(q_b^{sh} + q_d^{sh}\right)\right] \quad (13)$$

$$\min C = K \times L \times H \times P \quad (14)$$

$$s.t. K \times H \times cos\beta + (K-1) \times D \leq W \quad (15)$$

$$H + E \leq A_{max} \quad (16)$$

Variable bounds:

$$2 \leq K \leq 10 \quad (17)$$

$$0.2 \leq H \leq 2 \quad (18)$$

$$0^o \leq \beta \leq 90^o \quad (19)$$

$$0.8 \leq D \leq 2.5 \quad (20)$$

$$-45^o \leq \gamma_C \leq 45^o \quad (21)$$

$$0.5 \leq E \leq 2 \quad (22)$$

Where:

$$K \in Z^+$$

$$\$H, \beta, D, \gamma, E \in \mathrm{R}$$

- P is the price of PV panel per square meter.
- q_b is the yearly beam irradiation per unit area of an un-shaded collector (first row).
- q_d is the yearly diffuse irradiation per unit area of an un-shaded collector (first row).
- q_b^{sh} is the average yearly beam irradiation per unit area of shaded collectors$(n-1\,rows)$.
- q_d^{sh} is the average yearly diffuse irradiation per unit area of shaded collectors $(n-1\,rows)$.

3. ALGORITHMS AND SETTINGS

3.1 Multi-objective Optimization

Multi-objective optimization is the process of simultaneously optimizing two or more conflicting objectives subject to certain constraints. A multiobjective optimization problem may be defined as:

$$v_i = \begin{cases} min/\max\ F(x) = (F_1(x), F_2(x), \ldots, F_n(x)) \\ s.c\ x \in S \end{cases}$$

where $n\ (n \geq 2)$ is the number of objectives, $x = (x_1, \ldots, x_k)$ is the vector representing the decision variables, and S represents the set of feasible solutions associated with equality and inequality constraints and explicit bounds. $F(x) = (F_1(x), F_2(x), \ldots, F_n(x))$ is the vector of objectives to be optimized.

A large number of multi-objective metaheuristics were successfully used to solve real-life problems. Since 1960 there have been major developments in the metaheuristics field (Talbi, 2009).

The optimal solution for MOPs is not a single solution as for mono-objective problems, but a set of solutions defined as Pareto optimal solutions. A solution is Pareto optimal if it is not possible to improve a given objective without deteriorating at least another objective. The main goal of the resolution of a multiobjective problem is to obtain the Pareto optimal set and, consequently, non-dominated solutions known as the Pareto front.

An objective vector $\$u = (u_1, \ldots, u_n)$ is said to $dominate\ v = (v_1, \ldots, v_n)$ (denoted by $u \prec v$ if and only if no component of v is smaller than the corresponding component of u and at least one component of u is strictly smaller, assuming a minimization problem, that is,

$\forall\, i \in \{1, \ldots, n\}: u_i \leq v_i \wedge \exists\, i \in \{1, \ldots, n\} : u_i < v_i$

3.2 NSGA-II

It is a popular fast elitist multi-objective, non-domination based genetic algorithm (Deb et al, 2012). NSGA-II is able to find well spread solutions over the Pareto-optimal front and requires low computational complexity $O(mN^2)$, where m is the number of objectives and N is the population size. The main components of NSGA-II are: elite-preserving operator (preserve and use previously found best solutions in subsequent generations), non-dominated sorting (population is sorted into a hierarchy of sub-populations based on the ordering of Pareto dominance) and crowded tournament selection operator to preserve the diversity among non-dominated solutions in the later stage of the run in order to obtain a good spread of solutions. NSGA-II algorithm and parameter settings used in all our experiments are presented in Algorithm 1 and Table I, respectively.

Algorithm 1: NSGA-II Algorithm

```
Generate initial population (uniform random distribution);
Evaluate objective values
Assign rank (level) based on Pareto dominance
Generate child population
    Tournament selection
    Recombination and mutation
for i = 1 to number of generations do
    for all Parent and child population do
        Assign rank based on Pareto
        Generate sets of non-dominated fronts
        Determine the crowding distance
        between points on each front
    end for
    Select elitist points based on rank and
    crowding distance
    Create next generation
        Tournament Selection
        Recombination and Mutation
end for
```

Table I. NSGA-II parameters' setting.

Population size	100
Initial population	Uniform Random
Maximum Function Evaluation	10^5
Mutation probability	1/6[1]
Crossover probability	0.9
Mutation distribution Index	20
Crossover distribution Index	20
Number of Runs	100

3.3 GDE3

GDE3 is an extension of Differential Evolution (DE) for global optimization with an arbitrary number of objectives and

[1] The number 6 represents the dimension of the problem

constraints (Kukkonen & Lampinen, 2005). GDE3 with a single objective and without constraints is similar to the original DE. GDE3 improves earlier GDE versions in the case of multi-objective problems by giving better distributed solutions. GDE3 modifies earlier GDE versions using a growing population and non-dominated sorting with pruning of non-dominated solutions to decrease the population size at the end of each generation. This improves obtained diversity and makes the method more stable for the selection of control parameter values. GDE3 algorithm and parameter settings used in all our experiments are shown in Algorithm 2 and in Table II, respectively.

Algorithm 2: GDE3 Algorithm

Generate uniform random parent population of NP individuals.
Set $m = 0$
Evaluate objective values
for $i = 1$ to number of generations **do**
  for all Parent population **do**
    Evaluate objective values for the trial vector
    Selection process:

$$x_i, G+1 = \begin{cases} u_i, G+1, & if\ u_i, G+1 \preccurlyeq x_i, G \\ x_i, G & otherwise \end{cases}$$

    Set $m = m + 1, x_{NP+m}, G+1 = u_i, G+1$
    If $\forall j: gj(u_i, G+1) \leq 0 \wedge x_i, G+1 == x_i, G+1 \wedge u_i, G \preccurlyeq u_i, G+1$
  end for
  Create next generation
  Apply non-dominated ranking to $NP + m$ vectors. Select NP non-dominated vectors and set $m = 0$.
end for

Table II. GDE3 parameters' setting

Population size	100
Initial population	Uniform Random
Maximum Function Evaluation	10^5
Mutation probability	0.5
Crossover probability	0.9
Number of Runs	100

4. PHOTOVOLTAIC PARAMETERS

4.1 Climate Information

The location selected for all the experiments is Toronto, Ontario, Canada (Latitude 43.45^o/ Longitude -79.25^o). Appendix B, Tables VII and VIII show 30 years of monthly averaged hourly direct normal beam irradiance and horizontal diffuse irradiance in KWh/m^2 (NCDIA, 2012). These datasets were created by joining twelve Typical Meteorological Months selected from a database of 30 years of Canadian Weather Energy and Engineering Datasets (CWEEDS) data. Appendix B, Tables VII and VIII show the monthly averaged hourly direct and diffuse irradiance (used in equations 9 to 12) and tables IX and X show 22 years monthly averaged hourly solar angles relative to the horizon and solar azimuth angles due south in degrees (used in equations 5 and 7). The solar datasets were taken from the NASA GEOS-4 (NASA, 2012).

4.2 PV Panel Specification

There are numerous types of PV panels in the market. PV panels are priced based on their electrical characteristics (Rated power, Voltage, Current, Module efficiency, Short-circuit current, Open-circuit voltage, Maximum series fuse rating, Maximum system voltage) and mechanical characteristics (Dimensions, Weight, Frame, number of Solar Cells). For our experiment, we have used Ameresco Solar BP 90 Watt, 12Vsolar panel priced at \$616.59/m^2 (www, 2012). Please note that even though this specific solar panel was use for the experiments, the solution outcome would not necessarily be affected if other panels are used. In overall, the current PV panels' average price in Ontario is \$4.50 per Kwh including all installation fees and required material.

Figure 4. The best (HV) set of non-dominated solution set found by NSGA-II with respect to number of collector rows.

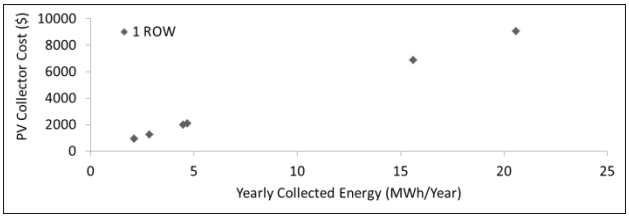

(a) 1 row

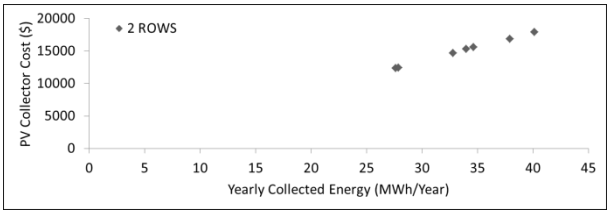

(b) 2 rows

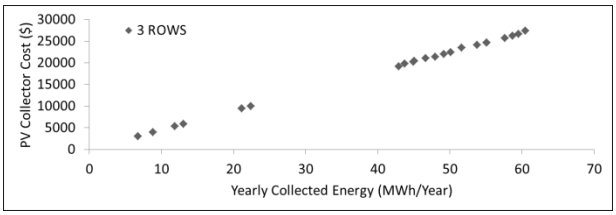

(c) 3 rows

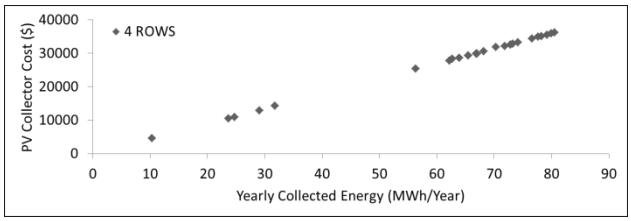

(d) 4 rows

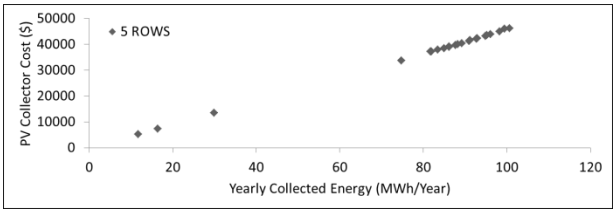

(e) 5 rows

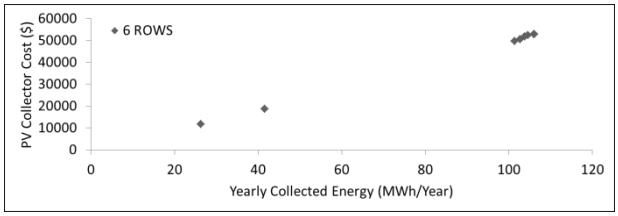

(f) 6 rows

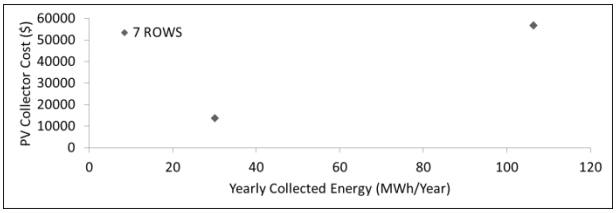

(g) 7 rows

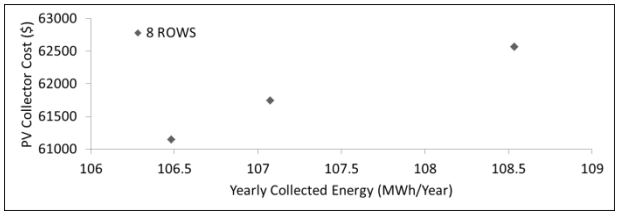

(h) 8 rows

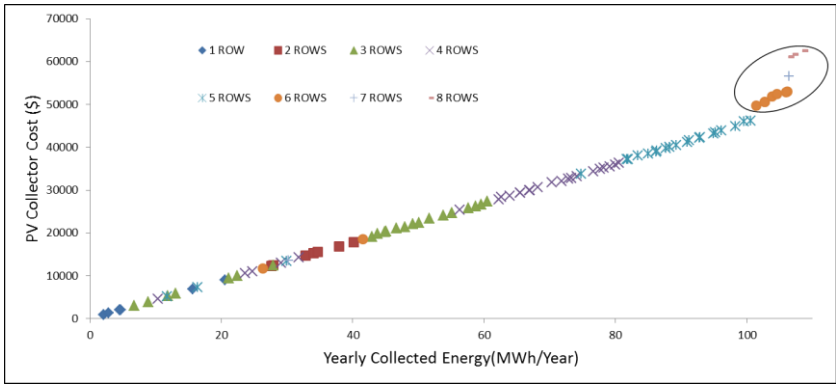

(i) All rows

5. RESULTS AND DISCUSSION

Due to stochastic nature of MOEAs, NSGA-II, and GDE3 were executed 100 times each independently. The stopping criteria for both algorithms is 10^5 function evaluations. Their best and median solutions were compared graphically. In addition, the hypervolume (HV) measure (Zitzler & Thiele, 1999) was used for complementarity; the Wilcoxon statistical procedure (www, 2012) was used to present the HV results at a 0.05 significance level. The HV measure or S metric is described as the Lebesgue measure Λ of the union of hypercubes a_i defined by a non-dominated point m_i and a reference point x_{ref}:

$$S(M) := \Lambda\ (\bigcup_i a_i | m_i \in M\ ) = \Lambda\left(\bigcup_{m \in M} x | m \prec\ x \prec\ x_{ref}\right)$$

There were notable differences among the best solutions found by NSGA-II and GDE3. The most important difference consisted in NSGA-II being able to find a more complete spectrum of the Pareto front. Hence, a section of Pareto front is completely missed by GDE3. This missed section by GDE3 is circled in Fig. 6.

If that missed section of the solutions is ignored, it can be seen that found solutions are similar. However, there is a difference in term of mapping. As explained earlier, the studied problem has many-to-one mapping properties that makes more complex. I.e., different setup parameters can generate the same solutions. For example, one row of very large PV panels can generate the same amount of energy as 6 rows of small PV panels. To illustrate the different setups based on the number of rows, the solutions found respectively by NSGA-II and GDE3 are show in Fig. 4 and Fig. 5.

To do a comparison from a more neutral angle, the respective Pareto sets of NSGAII and GDE3 are shown in Figs. 7 and Fig. 8 based on their median HV measure. It can be seen that the solutions found are very similar; the Pareto set geometry is very similar as shown in Fig 9. However, the parameters are different as shown in Fig. 7 and Fig. 8.

On the other hand, GDE3 had a better dispersion of found candidate solutions than NSGA-II. As shown in Fig. 5, the solutions in the objective space of GDE3 are more evenly distributed as compared to NSGA-II as shown in Fig. 4. It can be seen, as pointed out, a different location of Pareto front found by NSGA-II, there are small gaps and other more compact areas. However, this deficiency is less important as compared to the problem described in the previous paragraph because the real Pareto front can be estimated. For example, approximation methods can be used to complete these gaps. Otherwise, the optimization can continue further with emphasis on those sections which are in the interest of decision makers (such as what is done with interactive multi-objective optimizers). Tables III and IV show the best (HV) set of non-dominated solution set found by NSGA-II and GDE3 algorithms.

When comparing the decision variables, for example, the number of collector rows K, and the collector's inclination angle (β), GDE3's solutions were not as diverse as NSGA-II. Fig. 5f shows the only one (GDE3 could not jump to the a higher inclination angle) solution with $K = 6$ that is found using GDE3 however Fig. 4f, g, and h show that there are 9 solutions corresponding to $K = 6$, 3 solutions with $K = 7$, and 4 solutions with $K = 8$. NSGA-II was able to jump to higher inclination angles that satisfy problem constraints - from $\beta = 22.6$ to $\beta = 46.1$, which resulted with the energy $Q = 106.15$ MWh/year.

Figure 5. The best (HV) set of non-dominated solution set found by GDE3 with respect to number of collector rows

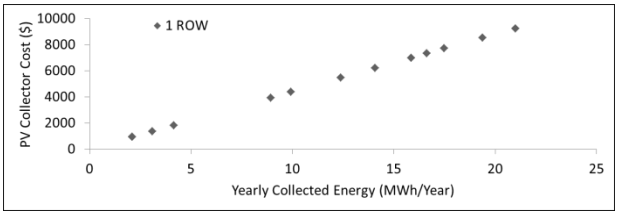

(a) 1 row

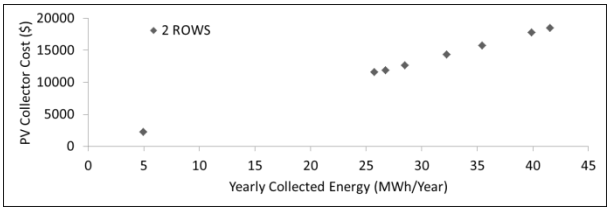

(b) 2 rows

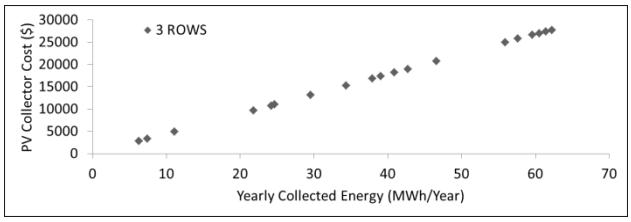

(c) 3 rows

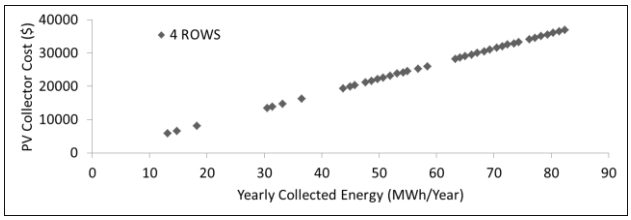

(d) 4 rows

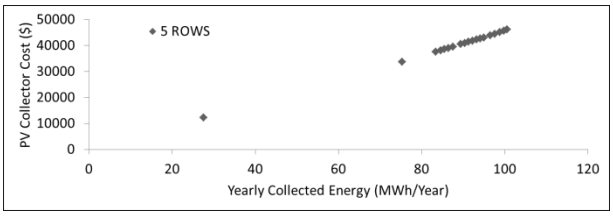

(e) 5 rows

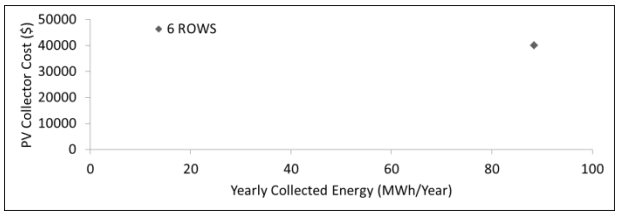

(f) 6 rows

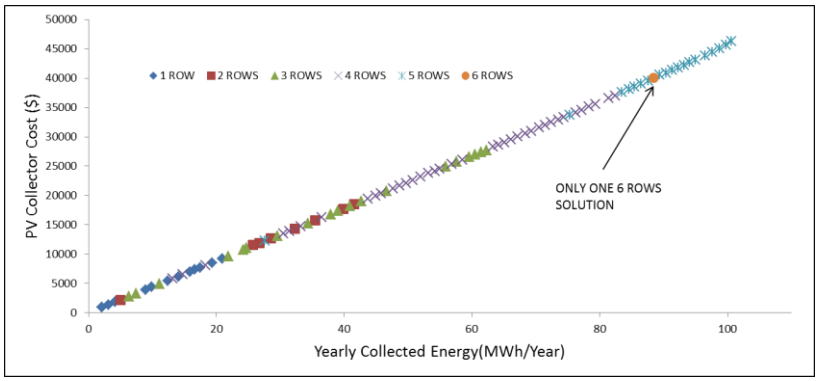

(g) All rows

Figure 6. The non-dominated solution set found by NSGA-II and GDE3 algorithms based on their respective best HV measure.

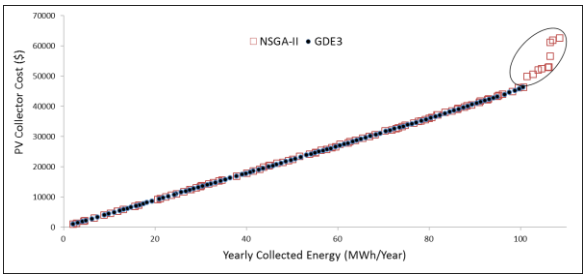

Figure 7. The non-dominated solution set found by NSGA-II based on the HV median.

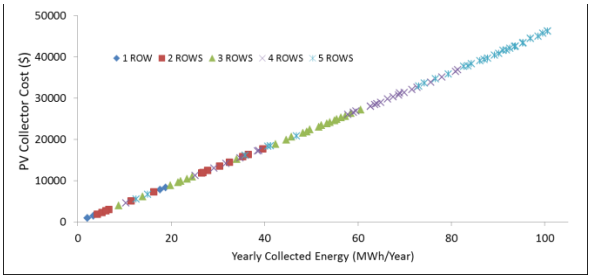

Another interesting observation as pointed in Fig. 5 is that the GDE3 solutions are different. For example, solutions with 2 rows are right beside of solutions with 6 rows in the objective space. Despite their very different configuration two rows with large dimensions and large space between rows vs. six rows with small dimensions and tight spaces between rows, the energy output was very similar. Therefore, GDE3 has strong Many-to-one mapping properties because NSGA-II was unable to find such energy outputs with large number of rows.

Figure 8. The non-dominated solution set found by GDE3 based on the HV median.

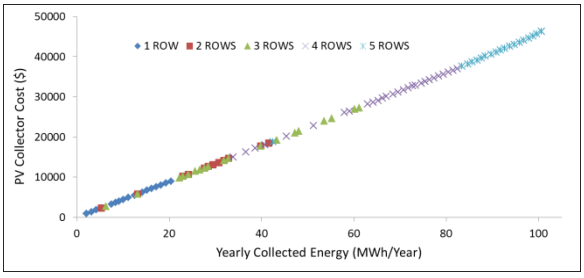

Figure 9. The non-dominated solution sets found by NSGA-II and GDE3 algorithms based on the median HV.

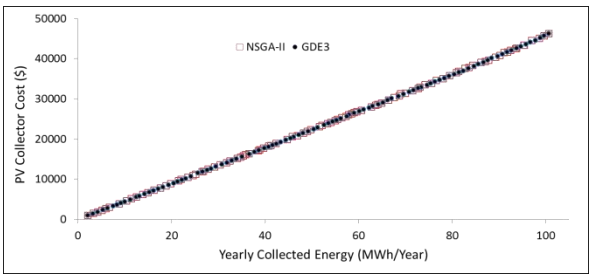

One extreme solution of the Pareto optimal solution consists in having the minimal investment that generates the lowest absorbed energy. It is the lowest possible cost. The other extreme of the Pareto optimal solution consists in having the maximum energy (over 108 MWh/year) with the maximum investment (over $60,000). The use of multi-objective optimizers generated solutions that would not be found using single objective optimizations. In Fig. 3, it can be observed that there is a linear relationship between the two cost and energy absorbed objectives with these respective ranges $C = [924.88, 46{,}236.00]$ and $Q = [2.10, 100.63]$ MWh/year. Past, the $C = 46{,}236.00$ and $Q = 100.63$ MWh/year, the linear relationship have a higher slope (i.e. the return on investment (ROE)) becomes less attractive to decision makers. For example, if an investor has comfortable amount of money and is looking into maximizing his ROE, probably he will select the solution $C = \$46{,}236.00$ and $Q = 100.63$ MWh/year. Other solutions with lower investment can also be selected if the investor has budget limitations by preserving the same ratio of ROE.

The Table V show the average HV with the standard deviation. The Table VI show the median HV measure with the IQR. In both cases, the NSGA-II algorithm outperforms the GDE3 algorithms probably

Table III. The best (HV) set of non-dominated solution set found by NSGA-II.

K	H (m)	β $(^o)$	D (m)	γ $(^o)$	E (m)	Q (MWh)	Cost ($)
1	0.2	27.9	1.9	-4.0	0.6	2.1	924.9
1	0.2	27.9	1.8	-4.0	0.6	2.1	924.9
1	2.0	26.7	1.6	-3.9	0.6	20.6	9075.6
1	0.3	29.8	2.2	-4.0	0.6	2.8	1252.0
1	0.5	37.3	1.6	-3.9	0.5	4.7	2087.3
1	0.4	24.3	1.7	-3.9	0.5	4.5	1981.4
1	1.5	27.9	1.9	-4.0	0.5	15.6	6881.4
2	1.6	22.9	1.0	-3.9	0.6	32.8	14697.8
2	1.9	26.1	1.7	-3.9	0.6	40.1	17901.7
2	1.7	24.9	0.8	-5.1	0.9	34.0	15285.0
2	1.8	25.2	1.8	-3.9	0.5	37.9	16882.7
2	1.3	28.9	1.6	-1.4	0.6	27.6	12346.3
2	1.7	21.1	1.0	-2.7	0.5	34.7	15582.4
2	1.3	27.0	1.8	-7.6	0.6	27.9	12428.6
3	0.2	28.0	2.2	-15.8	0.5	6.8	2981.9
3	2.0	16.4	1.4	-3.8	0.5	60.5	27360.7
3	1.5	36.4	2.3	-15.8	0.5	46.7	21062.7
3	0.7	25.3	2.2	-15.4	0.5	22.4	9937.0
3	1.5	26.0	2.2	-4.0	0.5	48.0	21346.7
3	1.4	23.4	1.8	-14.2	0.6	42.9	19178.1
3	1.6	26.5	1.6	-3.1	0.7	49.2	22046.7
3	1.9	22.3	1.9	-3.9	0.6	57.6	25749.1
3	1.4	26.2	1.9	0.8	0.6	43.7	19770.5
3	1.9	25.9	1.9	-3.9	0.5	59.5	26602.6
3	1.6	22.0	1.8	-3.8	1.2	50.1	22429.3
3	1.9	25.9	1.9	-3.9	0.6	58.7	26232.1
3	0.7	24.9	1.0	-5.1	0.9	21.2	9432.9
3	1.5	26.2	1.9	0.8	0.6	45.1	20381.6
3	1.7	25.3	1.9	-12.8	0.5	53.8	24069.3
3	0.3	28.4	0.8	-4.0	0.6	8.9	3928.2
3	1.8	25.3	2.1	-15.4	0.5	55.1	24630.6
3	1.7	18.2	0.8	-16.0	0.5	51.7	23438.2
3	0.4	21.0	1.0	-14.1	0.6	13.1	5842.6
3	1.5	21.3	1.0	-4.2	0.8	44.9	20231.9
3	1.8	26.3	2.1	-15.4	0.6	55.1	24613.4
4	1.7	25.2	1.6	-6.4	0.6	68.2	30590.0
4	1.7	34.2	1.8	-15.8	0.6	70.3	31849.0
4	0.3	28.4	0.8	-4.0	0.6	10.3	4577.3
4	1.9	22.1	1.6	-3.8	0.6	76.6	34343.4
4	0.6	28.7	2.3	-3.9	0.6	24.7	10944.2
4	0.8	25.6	0.9	-14.8	0.5	31.8	14232.6
4	1.4	23.4	1.8	-20.9	0.5	56.3	25359.9
4	0.6	28.7	0.8	-3.9	0.6	23.6	10555.2
4	2.0	26.7	1.4	-3.9	0.8	80.5	36302.5
4	0.7	26.7	1.6	-4.1	0.7	29.1	12940.1
4	1.7	24.9	1.8	-3.9	0.6	71.9	32135.5
4	1.5	24.1	1.8	-4.9	0.7	62.2	27831.8
4	1.6	28.0	1.9	-3.8	0.6	63.9	28622.3
4	1.9	28.5	1.8	-4.4	0.5	77.7	34957.9
4	1.8	24.9	1.8	-2.9	0.6	74.1	33240.7
4	1.9	22.6	1.6	-5.5	0.6	79.2	35559.9
4	1.5	28.0	1.7	-9.7	0.6	62.7	28312.7
4	1.6	25.2	1.6	-6.4	0.6	65.5	29364.3
4	1.9	22.6	1.5	-4.0	0.5	80.0	35913.4
4	1.8	27.9	1.9	-3.9	0.7	72.8	32609.4
4	1.9	24.1	1.7	-6.4	0.6	78.3	35145.0
4	1.6	25.2	1.6	-6.4	0.6	65.5	29364.3
4	1.6	22.1	1.8	-3.9	1.2	66.9	29905.8
4	1.6	22.1	1.8	-3.9	0.5	67.0	29957.2
4	1.8	24.9	1.7	-3.9	0.6	73.3	32816.9
5	0.3	27.9	0.8	-10.4	0.6	16.4	7338.9
5	2.0	28.4	0.8	-4.0	0.6	100.6	46236.0
5	1.9	26.1	0.8	-3.9	0.6	98.2	44874.4
5	1.9	25.7	0.8	-14.3	0.6	96.1	43921.0
5	1.6	15.6	0.8	-4.2	0.6	83.5	37987.0
5	2.0	28.4	0.8	-21.9	0.6	99.5	46050.3
5	1.7	21.1	1.0	-4.0	0.6	85.0	38450.3
5	1.5	25.9	1.0	-4.0	0.6	74.8	33719.8
5	1.8	22.1	0.8	-3.9	0.6	91.0	41257.3
5	1.8	26.5	0.9	-3.9	0.7	92.9	42337.4
5	1.7	21.1	1.0	-4.0	0.8	87.7	39710.6
5	1.8	22.1	0.9	-4.0	1.2	89.3	40417.4
5	1.8	25.5	0.8	-4.7	0.8	91.2	41622.4
5	1.6	24.8	0.8	-3.9	1.1	81.9	37178.1
5	1.8	22.1	0.9	-4.3	1.1	92.8	42156.8
5	1.6	25.9	0.8	-3.9	0.6	81.7	37146.3
5	0.2	22.1	0.8	-4.2	0.6	11.7	5225.9
5	1.7	22.1	0.8	-16.0	0.7	86.3	39196.4
5	1.7	21.1	1.0	-4.0	0.6	86.2	38956.0
5	1.9	22.1	0.8	-4.2	0.6	94.9	43180.4
5	1.9	25.6	0.9	-14.3	0.6	95.3	43476.3
5	1.7	21.1	0.8	-15.8	0.5	88.3	40110.1
5	0.6	21.9	0.8	-16.7	0.6	30.0	13437.2
6	1.8	43.4	0.8	-4.7	0.7	101.4	49768.7
6	1.9	46.1	0.8	-14.3	0.6	106.2	52962.0
6	0.4	30.4	1.6	-14.1	0.6	26.3	11685.1
6	1.9	46.2	0.8	-10.9	0.6	103.8	51911.8
6	0.7	22.6	0.8	-4.1	1.1	41.5	18614.8
6	1.9	46.5	0.8	-3.9	0.6	104.6	52458.0
6	1.8	43.9	0.8	-3.9	0.6	102.7	50514.5
6	1.9	46.1	0.8	-14.3	0.6	106.0	52874.1
6	1.8	43.9	0.8	-3.9	0.6	102.7	50514.5
7	1.8	54.2	0.8	-16.0	0.5	106.5	56581.0
7	1.8	54.2	0.8	-16.0	0.5	106.5	56581.0
7	0.4	30.4	0.8	-18.1	0.6	30.2	13632.6
8	1.7	61.9	0.8	-16.0	0.5	108.5	62563.4
8	1.7	61.9	0.8	-16.0	0.5	108.5	62563.4
8	1.7	61.8	0.8	-16.0	0.5	106.5	61142.4
8	1.7	62.0	0.8	-16.0	0.5	107.1	61741.8

because of the missed portion of Pareto Set by GDE3. However, GDE3 shows a better consistence in the results because of a smaller standard deviation and IQR than NSGA-II.

Table IV. The best (HV) set of non-dominated solution set found by GDE3.

K	H (m)	β $(^o)$	D (m)	γ $(^o)$	E (m)	Q (MWh)	Cost ($)
1	1.9	26.6	1.7	-4.0	0.6	19.4	8538.4
1	1.0	26.3	2.2	-4.0	0.6	9.9	4373.1
1	0.3	26.3	0.8	-4.0	1.3	3.1	1367.3
1	1.6	23.2	1.8	-4.0	0.5	16.6	7341.1
1	0.2	28.0	0.8	-4.0	1.2	2.1	924.9
1	1.3	27.1	0.8	-4.0	1.0	14.1	6199.2
1	0.2	28.0	0.8	-4.0	0.5	2.1	924.9
1	1.5	27.0	2.5	-4.0	1.1	15.9	6992.9
1	0.9	24.4	1.8	-4.0	0.5	8.9	3937.7
1	2.0	27.7	0.8	-4.0	0.9	21.0	9248.8
1	1.2	28.9	2.3	-4.0	0.5	12.4	5458.2
1	0.4	26.7	2.1	-4.0	0.5	4.2	1829.6
1	1.7	27.1	1.0	-3.9	0.6	17.5	7708.2
2	1.3	24.3	1.7	-4.0	0.8	26.8	11887.5
2	1.6	24.1	2.5	-3.9	0.5	32.3	14323.9
2	1.7	27.5	2.4	-4.0	0.7	35.5	15754.7
2	1.3	27.7	0.8	-4.0	0.9	25.8	11552.7
2	2.0	21.9	2.5	-4.0	0.9	41.6	18497.6
2	1.9	27.3	2.5	-4.0	0.9	39.9	17738.5
2	1.4	23.2	2.2	-4.0	0.5	28.5	12654.8
2	0.2	26.4	2.5	-4.0	0.5	5.0	2194.0
3	1.1	25.6	2.5	-3.9	0.8	34.4	15250.8
3	0.7	26.5	2.5	-4.0	0.6	21.8	9668.8
3	1.8	23.8	1.8	-4.0	0.5	55.9	24971.8
3	0.2	27.8	2.5	-4.0	0.7	6.3	2774.7
3	2.0	22.7	2.5	-4.0	1.1	61.4	27379.4
3	1.0	23.6	2.0	-4.0	0.6	29.5	13119.2
3	0.8	21.6	0.9	-4.0	0.7	24.7	11039.3
3	0.8	26.3	1.8	-4.0	0.9	24.2	10751.0
3	1.9	23.4	2.1	-4.0	0.9	57.6	25760.6
3	1.9	26.8	2.5	-4.0	0.5	60.5	26981.1
3	1.3	25.4	2.0	-4.0	1.0	39.1	17369.4
3	1.4	26.5	2.4	-4.0	1.2	42.7	18979.6
3	1.3	26.5	2.3	-4.0	1.2	40.9	18165.3
3	1.9	25.1	2.0	-4.0	0.9	59.6	26607.8
3	0.2	26.4	2.0	-4.0	0.8	7.5	3291.1
3	1.5	26.9	2.3	-4.0	0.6	46.6	20740.0
3	0.4	25.5	2.5	-4.0	0.6	11.1	4911.8
3	1.2	25.5	2.5	-4.0	0.6	37.9	16828.8
3	2.0	25.2	2.5	-4.0	1.0	62.3	27746.5
4	1.1	25.6	2.5	-3.9	0.8	45.8	20334.4
4	1.9	24.3	1.7	-4.0	0.8	77.2	34573.6
4	1.9	23.5	1.7	-4.0	0.6	76.2	34153.5
4	1.9	24.5	1.7	-4.0	0.5	79.4	35575.6
4	1.8	23.8	1.7	-4.0	0.8	74.4	33295.7
4	1.6	23.6	1.5	-4.0	0.5	67.1	30059.3
4	1.1	25.5	2.4	-4.0	0.6	44.9	19953.0
4	1.7	23.5	1.8	-4.0	0.5	71.5	31964.9
4	1.6	23.6	1.7	-4.0	1.3	65.1	29070.3
4	1.3	24.0	1.8	-4.0	1.3	54.2	24177.5
4	1.8	23.6	1.7	-4.0	1.3	73.5	32909.1
4	0.4	24.8	1.7	-4.0	1.3	18.3	8099.8
4	1.3	24.3	1.7	-4.0	0.5	52.0	23167.0
4	0.8	24.3	2.5	-4.0	0.5	33.2	14740.6
4	1.4	25.8	2.3	-4.0	1.2	58.5	26037.0
4	1.7	24.0	2.0	-4.0	0.6	68.4	30519.1
4	1.6	24.0	2.0	-4.0	0.6	66.1	29517.2
4	2.0	22.5	1.5	-4.0	0.6	81.4	36541.1
4	1.1	25.0	2.5	-4.0	0.9	47.7	21169.5
4	1.6	24.1	1.7	-4.0	0.6	64.1	28647.7
4	0.3	23.1	1.6	-4.0	0.5	13.1	5825.9
4	2.0	22.5	1.5	-4.0	0.6	82.4	36995.3
4	1.8	27.0	1.5	-4.0	1.1	72.4	32552.5
4	1.7	24.0	1.7	-4.0	1.1	69.3	31007.6
4	1.3	26.4	1.3	-4.0	1.1	53.2	23798.0
4	1.9	21.6	1.5	-4.0	1.2	78.3	35137.1
4	1.7	24.2	1.5	-4.0	0.5	70.5	31616.6
4	1.2	24.7	2.5	-4.0	1.0	48.7	21633.4
4	1.5	25.9	1.8	-4.0	0.9	63.3	28268.1
4	0.7	26.8	2.5	-4.0	0.5	30.5	13505.8
4	1.2	23.6	1.9	-4.0	1.2	50.7	22584.7
4	1.1	24.6	2.3	-4.0	1.2	43.7	19421.9
4	0.8	27.4	2.5	-4.0	0.8	31.4	13931.7
4	1.4	23.2	2.2	-4.0	0.7	56.8	25309.6
4	1.2	27.2	2.5	-4.0	0.6	49.8	22108.2
4	1.3	22.6	2.2	-4.0	0.6	55.0	24499.3
4	0.9	23.9	1.9	-4.0	1.2	36.5	16217.9
4	0.4	24.2	2.1	-4.0	0.8	14.8	6549.1
4	2.0	22.3	1.6	-4.0	0.6	80.4	36069.8
5	1.9	20.0	0.8	-4.0	0.5	94.9	43091.6
5	1.9	19.7	0.8	-4.0	0.6	94.1	42694.8
5	0.5	23.1	1.6	-4.0	0.8	27.6	12254.6
5	1.9	24.5	0.8	-4.0	0.8	97.6	44469.5
5	1.7	21.4	1.0	-4.0	1.0	86.5	39022.7
5	2.0	28.6	0.8	-4.0	0.6	100.6	46244.1
5	1.6	23.6	1.1	-4.0	0.6	83.4	37574.2
5	1.5	22.8	1.3	-4.0	0.5	75.3	33775.4
5	1.8	22.5	0.9	-4.0	0.9	90.4	40914.8
5	1.8	21.6	0.9	-4.0	1.0	93.2	42223.9
5	2.0	27.1	0.8	-3.9	0.6	99.7	45676.4
5	1.8	21.6	0.9	-4.0	0.5	91.3	41383.3
5	1.7	21.2	1.0	-4.0	0.5	87.5	39520.7
5	1.7	21.2	1.1	-4.0	0.5	84.6	38116.1
5	1.8	20.2	0.8	-4.0	0.7	89.4	40533.2
5	1.9	21.9	0.8	-4.0	0.8	96.5	43842.9
5	1.7	22.7	1.0	-4.0	0.6	85.4	38540.8
5	1.8	20.3	0.9	-4.0	0.5	92.2	41785.3
5	2.0	25.6	0.8	-4.0	0.8	98.7	45087.3
6	1.4	22.5	0.8	-4.0	0.5	88.4	40013.2

Table V. HV Mean and Standard Deviation

	NSGA-II	GDE3
PV	$2.36e+09_{4.0e+08}$	$2.41e+09_{1.0e+06}$

Table VI. HV Median and IQR

	NSGA-II	GDE3
PV	$2.40e+09_{4.8e+06}$	$2.41e+09_{1.2e+06}$

6. CONCLUSIONS

In this paper, two state-of-the art MOEAs, namely NSGA-II and GDE3, were used for optimal deigning of solar farm. The objectives were the maximization of the total incident solar energy and the minimization of the cost of deployment for a specific field. The decision variables consisted in number of collector rows, distance between collector rows, dimension of collectors, collectors inclination angle and collectors azimuth.

The proposed MOO optimization methods permitted to find a variety of optimal PV farm design solutions which would not be found using single objective solutions. For example, some intermediate solutions could be of interest with regards to other non-expressed objectives or secondary objectives such as space between solar panels or other technical aspects. Based on our result the maximum energy was $Q = 108.54$ MWh/year when the number of rows $K = 8$, the PV panel height $H = 1.69\ m$, the PV inclination angle $\beta = 61.2^{o}$, the distance between subsequent panels $D = 80\ cm$, and the PV clearance above the ground $E = 51\ cm$.

Our results showed that overall NSGA-II had a better performance than GDE3 because it was able a broader spectrum of the Pareto front. NSGA-II has found a portion of the Pareto front that was not found by GDE3. GDE3 had a slightly better distribution of the non-dominated solutions as compared to NSGA-II and had a better many-to-one mapping properties.

The generated solutions demonstrated the practicality of MOEAs which generated interesting solutions with a higher ROI in the middle of the Pareto front which won't be generated using a single objective optimization method.

As future work, we would like to extend the deployment of solar farms with tracking capability as supposed to stationary solar farms discussed in this paper. Also, we would like to investigate gradual linear land inclination between rows to minimize the shadow on subsequent rows. Finally we would like investigate the use of ray focusing mirrors to direct the radiation when the sun's ray is not in the direction of the solar panels.

ACKNOWLEDGEMENTS

The authors wish to thank Dr. Sophie Pelland from the Natural Sciences and Engineering Research Council (NSERC) for her precious help in clarification regarding NSERC meteorological data.

REFERENCES

Bourennani F., Rizvi R., & Rahnamayan S. (2010). Optimal Photovoltaic Solar Power Farm Design using the Differential Evolution Algorithms, *International Conference on Clean Energy (ICCI'10), Gazimagusa*, N. Cyprus, ref. 7-20, pp. 1-8.

Chang Y.(2010), Optimal the tilt angles for photovoltaic modules in Taiwan, *International Journal of Electrical Power & Energy Systems*, Volume 32, Issue 9, pp. 956-964.

Deb K., Ruiz F., Luque M., Tewari R., Cabello J. M., & Cejudo J. M. (2012), On the sizing of a solar thermal electricity plant for multiple objectives using evolutionary optimization, *Applied Soft Computing*, Volume 12, Issue 10, pp. 3300-3311.

Deb K., Pratap A., Agarwal S. & Meyarivan T. (2002), A fast and elitist multiobjective

genetic algorithm: NSGA-II, *Evolutionary Computation, IEEE Transactions*, vol.6, no.2, pp.182-197.

Ekren O. & Ekren B. Y. (2010), Size optimization of a PV/wind hybrid energy conversion system with battery storage using simulated annealing, *Applied Energy*, Volume 87, Issue 2, pp. 592-598.

Huband S., Hingston P., Barone L. & While L. (2006), A review of multiobjective test problems and a scalable test problem toolkit, *IEEE Transaction on Evolutionary Computation*, vol. 10, pp.477-486.

Kukkonen S. & Lampinen J. (2005), GDE3: the third evolution step of generalized differential evolution, Evolutionary Computation, *2005 IEEE Congress on Evolutionary Computation*, vol.1, pp.443-450.

Mellit A., Kalogirou S.A., Hontoria L. & Shaari S. (2009), Artificial intelligence techniques for sizing photovoltaic systems: A review, *Renewable and Sustainable Energy Reviews*, Vol. 13, n. 2, pp. 406-419.

Myers B., Bernardi M. & Grossman J. C. (2010), Three-dimensional photovoltaics, *Applied Physics Letters*, Vol. 96.

Price H., Lüpfert E., Kearney D., Zarza E., Cohen G., Gee R. & Mahoney R. (2002), Advances in parabolic trough Solar power technology, *Journal of Solar Energy Engineering*, vol. 124, no2, pp. 109-125.

Sadineni S., Boehm R. & Hurt R. (2008), Spacing Analysis of an Inclined Solar Collector Field, *ASME 2nd International Conference on Energy Sustainability*, Jacksonville, Florida.

Schlaich J., Bergermann R., Schiel W. & Weinrebe G. (2005), Design of Commercial Solar Updraft Tower Systems—Utilization of Solar Induced Convective Flows for Power Generation, *Journal of Solar Energy Engineering*, pp. 117-125.

Sheskin D. J. (2007), *Handbook of Parametric and Nonparametric Statistical Procedures*, 4th ed, New York: Chapman & Hall/CRC Press.

Talbi E. (2009), *Metaheuristics from Design to Implematation*, John Wiley & Sons Publication Inc. pp.308-320.

Thiaux Y., Seigneurbieux J., Multon B. & Ben Ahmed H. (2010), Load profile impact on the gross energy requirement of stand-alone photovoltaic systems, *Renewable Energy*, Volume 35, Issue 3, pp. 602-613.

Varun S. (2010), Thermal performance optimization of a flat plate solar air heater using genetic algorithm, *Applied Energy*, 87 (5), pp. 1793–1799.

Weinstock D. & Appelbaum J. (2004), Optimal Solar Field Design of Stationary Collectors, *Journal of Solar Energy Engineering*, Vol. 126, pp. 898-905.

Weinstock D. & Appelbaum J. (2009), Optimization of Solar Photovoltaic Fields, *ASME Journal of Solar Energy Engineering*, Vol. 131.

Hongxing Y., Lin L. & Wei Z. (2007), A novel optimization sizing model for hybrid solar-wind power generation system, *Solar Energy*, Volume 81, Issue 1, pp. 76-84.

Zitzler E. & Thiele L. (1999), Multiobjective evolutionary algorithms: A comparative case study and the strength pareto approach, *Evolutionary Computation, IEEE Transaction*, Vol. 3, No. 4, pp. 257-271.

NCDIA (2012), Monthly Averaged Hourly Solar Angles Relative To The Horizon and Solar Azimuth Angles Due south in degrees. *National Climate Data and Information Archive* Retrieved August 3, from http://climat.meteo.gc.ca/prods_servs/index_e.html

NASA (2012), Monthly Averaged Hourly Solar Angles Relative To The Horizon(Degrees) and Monthly Averaged Hourly Solar Azimuth Angles(Degrees). *Atmospheric Science data center. NASA Surface meteorology and Solar Energy Information*, Retrieved August 3, 2012, from http://eosweb.larc.nasa.gov

www (2012) Solar Panels at Affordable Prices. *The Alternative Energy Store*, Retrieved August 3, 2012, from http://www.altestore.com/store/Solar-Panels/c541/

APPENDIX A

NOMENCLATURE

A_{max} = maximum collector height above ground
a_s = relative shaded area
D = distance between collector rows
D_{min} = minimum distance between collector rows
d = normalized distance between collector rows
F_d = configuration factor for un-shaded collectors
F_d^{sh} = configuration factor for shaded collectors
G_b = direct beam irradiance on the collector perpendicular to solar rays
G_{dh} = horizontal diffuse irradiance
H = collector height
H_s = shadow height
h_s = relative shadow height
H_{max} = maximum collector height
K = number of solar collector rows
L = solar field length
L_s = shadow length
l = normalized collector length
l_s = relative shadow length
Q = yearly energy
q_b = yearly beam irradiation per unit area of an un-shaded collector (first row)
q_d = yearly diffuse irradiation per unit area of an un- shaded collector (first row)
q_b^{sh} = average yearly beam irradiation per unit area of shaded collector ($(K-1)$ rows)
q_d^{sh} = average yearly diffuse irradiation per unit area of shaded collector ($(K-1)$ rows)
T_R = sun rise on the collector for the beam irradiance
T_S = sun set on the collector for the beam irradiance
T_{SR} = sun rise for the diffuse irradiance
T_{SS} = sun set for the diffuse irradiance
W = solar field width
W_{max} = maximum solar field width
Z^+ = natural number set
α = sun elevation angle
β = collector inclination angle
γ = difference between the sun and collector azimuth
γ_C = collector azimuth with respect to south
γ_S = sun azimuth with respect to south
θ = angle between the solar beam and the normal to the collector
ΔT = time interval

APPENDIX B

TABLES

Table VII. Monthly averaged hourly direct normal beam irradiance: Latitude 43.45^{o} */ Longitude* -79.25^{o}*(Kwh/m^2)*

Time	Jan	Feb	Mar	Apr	May	Jun	Jul	Aug	Sep	Oct	Nov	Dec
0:00	0.0000	0.0000	0.0000	0.0000	0.0000	0.0000	0.0000	0.0000	0.0000	0.0000	0.0000	0.0000
1:00	0.0000	0.0000	0.0000	0.0000	0.0000	0.0000	0.0000	0.0000	0.0000	0.0000	0.0000	0.0000
2:00	0.0000	0.0000	0.0000	0.0000	0.0000	0.0000	0.0000	0.0000	0.0000	0.0000	0.0000	0.0000
3:00	0.0000	0.0000	0.0000	0.0000	0.0000	0.0000	0.0000	0.0000	0.0000	0.0000	0.0000	0.0000
4:00	0.0000	0.0000	0.0000	0.0000	0.0000	0.0000	0.0000	0.0000	0.0000	0.0000	0.0000	0.0000
5:00	0.0000	0.0000	0.0000	0.0047	0.1467	0.1583	0.1481	0.0153	0.0000	0.0000	0.0000	0.0000
6:00	0.0000	0.0000	0.0157	0.1577	0.3369	0.2626	0.3119	0.2088	0.1339	0.0018	0.0000	0.0000
7:00	0.0000	0.0234	0.2203	0.2634	0.4185	0.3398	0.3781	0.3113	0.3508	0.1634	0.0173	0.0000
8:00	0.0939	0.1708	0.3429	0.3327	0.4887	0.3896	0.4438	0.3813	0.4098	0.2218	0.0572	0.0659
9:00	0.1796	0.2569	0.3795	0.3745	0.4609	0.4468	0.4807	0.4104	0.4506	0.2570	0.1045	0.1436
10:00	0.2627	0.3035	0.3546	0.4053	0.4430	0.4467	0.5061	0.4117	0.4401	0.3320	0.1753	0.2243
11:00	0.3075	0.3277	0.3287	0.4304	0.4369	0.4531	0.5313	0.3910	0.4126	0.3312	0.1804	0.2444
12:00	0.3193	0.3500	0.3615	0.4094	0.4189	0.4398	0.5115	0.4044	0.4388	0.3034	0.2146	0.2718
13:00	0.3112	0.3291	0.3097	0.3829	0.3665	0.4108	0.4417	0.3821	0.4557	0.2903	0.2041	0.2671
14:00	0.2777	0.3139	0.2867	0.3373	0.3548	0.3649	0.3760	0.3616	0.4058	0.3043	0.1816	0.1803
15:00	0.2312	0.3128	0.2617	0.3486	0.3073	0.3333	0.3492	0.3488	0.3314	0.2685	0.0903	0.1191
16:00	0.1149	0.2586	0.2118	0.3050	0.2622	0.3139	0.3437	0.3249	0.2570	0.1759	0.0244	0.0029
17:00	0.0000	0.0565	0.1342	0.2282	0.1894	0.2753	0.2803	0.2428	0.1505	0.0139	0.0000	0.0000
18:00	0.0000	0.0000	0.0000	0.0610	0.0922	0.1934	0.2078	0.1399	0.0143	0.0000	0.0000	0.0000
19:00	0.0000	0.0000	0.0000	0.0000	0.0055	0.0903	0.0740	0.0016	0.0000	0.0000	0.0000	0.0000
20:00	0.0000	0.0000	0.0000	0.0000	0.0000	0.0000	0.0000	0.0000	0.0000	0.0000	0.0000	0.0000
21:00	0.0000	0.0000	0.0000	0.0000	0.0000	0.0000	0.0000	0.0000	0.0000	0.0000	0.0000	0.0000
22:00	0.0000	0.0000	0.0000	0.0000	0.0000	0.0000	0.0000	0.0000	0.0000	0.0000	0.0000	0.0000
23:00	0.0000	0.0000	0.0000	0.0000	0.0000	0.0000	0.0000	0.0000	0.0000	0.0000	0.0000	0.0000

Table VIII. Monthly averaged hourly horizontal diffuse irradiance: Latitude 43.45^{o} */ Longitude* -79.25^{o}*(Kwh/m^2)*

Time	Jan	Feb	Mar	Apr	May	Jun	Jul	Aug	Sep	Oct	Nov	Dec
0:00	0.0000	0.0000	0.0000	0.0000	0.0000	0.0000	0.0000	0.0000	0.0000	0.0000	0.0000	0.0000
1:00	0.0000	0.0000	0.0000	0.0000	0.0000	0.0000	0.0000	0.0000	0.0000	0.0000	0.0000	0.0000
2:00	0.0000	0.0000	0.0000	0.0000	0.0000	0.0000	0.0000	0.0000	0.0000	0.0000	0.0000	0.0000
3:00	0.0000	0.0000	0.0000	0.0000	0.0000	0.0000	0.0000	0.0000	0.0000	0.0000	0.0000	0.0000
4:00	0.0000	0.0000	0.0000	0.0001	0.0012	0.0079	0.0048	0.0005	0.0000	0.0000	0.0000	0.0000
5:00	0.0000	0.0000	0.0004	0.0086	0.0281	0.0389	0.0322	0.0190	0.0029	0.0000	0.0000	0.0000
6:00	0.0000	0.0017	0.0156	0.0411	0.0701	0.0816	0.0647	0.0591	0.0368	0.0088	0.0003	0.0000
7:00	0.0049	0.0199	0.0483	0.0957	0.1220	0.1354	0.1033	0.1118	0.0786	0.0444	0.0156	0.0013
8:00	0.0280	0.0556	0.0967	0.1378	0.1657	0.1902	0.1443	0.1609	0.1160	0.0921	0.0526	0.0197
9:00	0.0686	0.0960	0.1439	0.1843	0.2215	0.2298	0.1782	0.2155	0.1595	0.1415	0.0986	0.0610
10:00	0.1056	0.1267	0.1752	0.2339	0.2605	0.2803	0.2083	0.2637	0.1977	0.1802	0.1278	0.0943
11:00	0.1282	0.1522	0.2018	0.2314	0.2779	0.3088	0.2373	0.2937	0.2267	0.1920	0.1351	0.1016
12:00	0.1331	0.1699	0.1868	0.2255	0.2909	0.3202	0.2673	0.2943	0.2199	0.2039	0.1316	0.0993
13:00	0.1223	0.1817	0.1875	0.2105	0.2927	0.3171	0.2858	0.2796	0.2015	0.1868	0.1128	0.0892
14:00	0.0936	0.1507	0.1721	0.1915	0.2654	0.2889	0.2783	0.2463	0.1907	0.1427	0.0813	0.0755
15:00	0.0608	0.1040	0.1390	0.1498	0.2040	0.2339	0.2409	0.1998	0.1535	0.1018	0.0460	0.0415
16:00	0.0320	0.0596	0.0930	0.1078	0.1601	0.1715	0.1764	0.1511	0.1008	0.0532	0.0156	0.0073
17:00	0.0063	0.0293	0.0393	0.0597	0.1022	0.1190	0.1194	0.0992	0.0493	0.0103	0.0012	0.0006
18:00	0.0000	0.0032	0.0068	0.0190	0.0475	0.0660	0.0682	0.0461	0.0098	0.0007	0.0000	0.0000
19:00	0.0000	0.0000	0.0002	0.0029	0.0030	0.0245	0.0279	0.0123	0.0009	0.0000	0.0000	0.0000
20:00	0.0000	0.0000	0.0000	0.0000	0.0001	0.0036	0.0038	0.0003	0.0000	0.0000	0.0000	0.0000
21:00	0.0000	0.0000	0.0000	0.0000	0.0000	0.0000	0.0000	0.0000	0.0000	0.0000	0.0000	0.0000
22:00	0.0000	0.0000	0.0000	0.0000	0.0000	0.0000	0.0000	0.0000	0.0000	0.0000	0.0000	0.0000
23:00	0.0000	0.0000	0.0000	0.0000	0.0000	0.0000	0.0000	0.0000	0.0000	0.0000	0.0000	0.0000

Table IX. Monthly averaged hourly solar azimuth angles due south (degrees): 43.45^o */ Longitude* -79.25^o

Time	Jan	Feb	Mar	Apr	May	Jun	Jul	Aug	Sep	Oct	Nov	Dec
0:00	n/a	n/a	n/a	n/a	n/a	n/a	n/a	n/a	n/a	n/a	n/a	n/a
1:00	n/a	n/a	n/a	n/a	n/a	n/a	n/a	n/a	n/a	n/a	n/a	n/a
2:00	n/a	n/a	n/a	n/a	n/a	n/a	n/a	n/a	n/a	n/a	n/a	n/a
3:00	n/a	n/a	n/a	n/a	n/a	n/a	n/a	n/a	n/a	n/a	n/a	n/a
4:00	n/a	n/a	n/a	n/a	n/a	n/a	n/a	n/a	n/a	n/a	n/a	n/a
5:00	n/a	n/a	n/a	n/a	-116.0	-119.5	-119.4	n/a	n/a	n/a	n/a	n/a
6:00	n/a	n/a	n/a	-100.0	-106.1	-109.8	-109.5	-103.8	n/a	n/a	n/a	n/a
7:00	n/a	n/a	-82.8	-89.8	-96.3	-100.4	-99.9	-93.8	-84.1	-75.0	n/a	n/a
8:00	-60.0	-66.0	-72.0	-80.0	-86.1	-90.6	-90.1	-83.3	-74.0	-64.0	-57.0	-55.0
9:00	-49.0	-55.0	-60.0	-67.0	-75.0	-80.0	-79.0	-72.0	-61.0	-51.0	-45.0	-44.0
10:00	-36.0	-42.0	-46.0	-52.0	-60.0	-66.0	-65.0	-57.0	-46.0	-37.0	-32.0	-32.0
11:00	-23.0	-27.0	-29.0	-33.0	-38.0	-44.0	-45.0	-37.0	-27.0	-20.0	-17.0	-18.0
12:00	-7.0	-10.0	-10.0	-8.0	-8.0	-11.0	-15.0	-11.0	-5.0	-1.0	-1.0	-3.0
13:00	8.0	8.0	11.0	18.0	25.0	27.0	21.0	18.0	18.0	17.0	15.0	12.0
14:00	23.0	25.0	31.0	41.0	50.0	54.0	49.0	43.0	38.0	34.0	30.0	26.0
15:00	37.0	40.0	48.0	58.0	68.0	72.0	68.0	61.0	54.0	49.0	43.0	39.0
15:00	49.0	53.0	61.0	72.0	81.0	84.0	81.0	74.0	68.0	61.0	55.0	51.0
17:00	60.0	65.0	73.0	83.0	91.0	95.0	92.0	86.0	79.0	72.0	n/a	n/a
18:00	n/a	n/a	84.0	94.0	101.0	104.0	102.0	96.0	90.0	n/a	n/a	n/a
19:00	n/a	n/a	n/a	n/a	111.0	114.0	111.0	106.0	n/a	n/a	n/a	n/a
20:00	n/a	n/a	n/a	n/a	n/a	n/a	n/a	n/a	n/a	n/a	n/a	n/a
21:00	n/a	n/a	n/a	n/a	n/a	n/a	n/a	n/a	n/a	n/a	n/a	n/a
22:00	n/a	n/a	n/a	n/a	n/a	n/a	n/a	n/a	n/a	n/a	n/a	n/a
23:00	n/a	n/a	n/a	n/a	n/a	n/a	n/a	n/a	n/a	n/a	n/a	n/a

Table X. Monthly averaged hourly solar Angles relative to the horizon (degrees): 43.45^o */ Longitude* -79.25^o

Time	Jan	Feb	Mar	Apr	May	Jun	Jul	Aug	Sep	Oct	Nov	Dec
0:00	n/a	n/a	n/a	n/a	n/a	n/a	n/a	n/a	n/a	n/a	n/a	n/a
1:00	n/a	n/a	n/a	n/a	n/a	n/a	n/a	n/a	n/a	n/a	n/a	n/a
2:00	n/a	n/a	n/a	n/a	n/a	n/a	n/a	n/a	n/a	n/a	n/a	n/a
3:00	n/a	n/a	n/a	n/a	n/a	n/a	n/a	n/a	n/a	n/a	n/a	n/a
4:00	n/a	n/a	n/a	n/a	n/a	n/a	n/a	n/a	n/a	n/a	n/a	n/a
5:00	n/a	n/a	n/a	n/a	0.3	2.9	0.6	n/a	n/a	n/a	n/a	n/a
6:00	n/a	n/a	n/a	3.5	10.4	12.7	10.4	5.7	n/a	n/a	n/a	n/a
7:00	n/a	n/a	4.9	14.3	21.1	23.2	20.9	16.4	10.8	4.4	n/a	n/a
8:00	1.4	6.9	15.5	25.1	32.0	34.1	31.8	27.2	21.4	14.5	7.3	2.4
9:00	10.1	16.3	25.4	35.6	42.7	44.9	42.6	37.8	31.4	23.6	15.7	10.6
10:00	17.4	24.3	34.1	44.9	52.7	55.3	52.9	47.6	40.1	31.1	22.3	17.2
11:00	22.7	30.3	40.8	52.2	60.9	64.2	61.8	55.6	46.5	36.1	26.7	21.7
12:00	25.4	33.7	44.3	56.0	65.2	69.3	67.2	59.9	49.5	38.0	28.3	23.6
13:00	25.3	33.7	44.1	55.0	63.4	67.7	66.4	59.1	48.2	36.4	26.9	22.6
14:00	22.3	30.6	40.0	49.5	56.7	60.5	60.0	53.5	43.0	31.6	22.6	18.9
15:00	16.8	24.6	33.1	41.2	47.3	50.7	50.6	44.9	35.1	24.3	16.0	12.9
16:00	9.4	16.7	24.2	31.3	36.8	40.1	40.1	34.8	25.5	15.3	7.7	5.2
17:00	0.5	7.3	14.1	20.6	26.0	29.2	29.2	24.0	15.1	5.3	n/a	n/a
18:00	n/a	n/a	3.5	9.8	15.2	18.5	18.4	13.2	4.3	n/a	n/a	n/a
19:00	n/a	n/a	n/a	n/a	4.8	8.3	8.0	2.5	n/a	n/a	n/a	n/a
20:00	n/a	n/a	n/a	n/a	n/a	n/a	n/a	n/a	n/a	n/a	n/a	n/a
21:00	n/a	n/a	n/a	n/a	n/a	n/a	n/a	n/a	n/a	n/a	n/a	n/a
22:00	n/a	n/a	n/a	n/a	n/a	n/a	n/a	n/a	n/a	n/a	n/a	n/a
23:00	n/a	n/a	n/a	n/a	n/a	n/a	n/a	n/a	n/a	n/a	n/a	n/a